Heme/Hydrogen Peroxide Reactivity: Formation of Paramagnetic Iron Oxophlorin Isomers by Treatment of Iron Porphyrins with Hydrogen Peroxide

Heather R. Kalish,[†] Lechosław Latos-Grażyński,[‡] and Alan L. Balch*[,†]

Contribution from the University of California, Davis, California 95616, and the Department of Chemistry, University of Wrocław, Wrocław, Poland

Received May 12, 2000. Revised Manuscript Received October 12, 2000

Abstract: Treatment of iron(II) porphyrins, $(py)_2Fe^{II}$(OEP), $(py)_2Fe^{II}$(EtioP), $(py)_2Fe^{II}$(DeuteroP), $(py)_2Fe^{II}$(MesoP), and $(py)_2Fe^{II}$(ProtoP), where OEP are the dianions of octaethylporphyrin, etio-1 porphyrin, deuteroporphyrin-IX dimethyl ester, mesoporphyrin-IX dimethyl ester, and protoporphyrin-IX dimethyl ester, with hydrogen peroxide in pyridine-d_5 at −30 °C in the strict absence of dioxygen is shown to result in clean oxygenation of the heme and the formation of oxophlorin complexes, $(py)_2$Fe(OEPO), $(py)_2$Fe(EtioPO), $(py)_2$Fe(DeuteroPO), $(py)_2$Fe(MesoPO), and $(py)_2$Fe(ProtoPO). Reactions have been monitored by ^{1}H NMR spectroscopy. The product oxophlorin complexes are stable as long as the samples are protected from exposure to dioxygen. The hyperfine shift patterns and the relative intensities of the individual resonances have been analyzed in terms of a model in which the location of the meso oxygen substituent dominates the pattern of spin density distribution. The resulting ^{1}H NMR spectra obtained from oxidation of the unsymmetrically substituted hemes, $(py)_2Fe^{II}$(DeuteroP), $(py)_2Fe^{II}$(MesoP), and $(py)_2Fe^{II}$(ProtoP), with hydrogen peroxide have been analyzed. These spectra show that the four isomeric oxophlorin products are formed in a nonrandom fashion. Solvent effects can produce a significant alteration in the regiospecificity of heme oxygenation.

Introduction

The reactivity of heme proteins and hemes themselves toward hydrogen peroxide is a significant process that contributes to biological utility of hemes.[1] Catalases are heme enzymes that are designed to destroy hydrogen peroxide through disproportionation. Peroxidases utilize hydrogen peroxide to generate highly oxidized hemes that are then used in substrate oxidation.[2] In both of these enzyme classes it is the Fe(III) state of the heme that interacts with hydrogen peroxide to generate ferryl intermediates.[3] While cytochrome P450 is designed to utilize dioxygen to oxidize substrates, it can also use hydrogen peroxide in a short-circuited path (the peroxide shunt) to effect the same transformations.[4] The reactions of hydrogen peroxide with heme model compounds, particularly with mesotetra(aryl)porphyrins, have been utilized to effect olefin epoxidation as well as hydrocarbon hydroxylation.[5] However, reactions of hydrogen peroxide with model hemes frequently are accompanied by bleaching and catalyst destruction. The results reported here investigate the earliest stages in the heme modification by hydrogen peroxide in cases where the porphyrin meso sites are not protected by the presence of aryl substituents.

Scheme 1. Heme Cleavage by Heme Oxygenase[a]

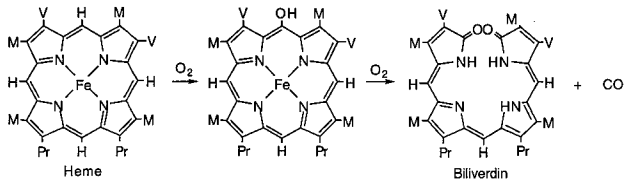

[a] Key: M = methyl; V = vinyl; Pr = propionate.

Biologically, heme degradation is catalyzed by the protein heme oxygenase, which utilizes heme as substrate to activate dioxygen to destroy the heme. This reaction results in the regiospecific cleavage of heme at the α-meso site as shown in Scheme 1.[6−9] This process generates the green tetrapyrrole, biliverdin, which is subsequently reduced by biliverdin reductase to bilirubin, the yellow pigment that is responsible for jaundice in humans. The iron is released as free iron ion, and the meso carbon atom is oxidized to carbon monoxide, a neurotransmitter.[10]

The regiospecificity of the reaction catalyzed by heme oxygenase is determined by the initial event, which involves attack of oxygen at the α-meso carbon. It is widely accepted that the first step in heme degradation by heme oxygenase results

[†] University of California.
[‡] University of Wrocław.

(1) Strukul, G., Ed. *Catalytic Oxidations with Hydrogen Peroxide as Oxidant*; Kluwer Academic Publishers: Boston, 1992.
(2) Everse, J.; Everse, K. E.; Grisham, M. B. *Peroxidases in Chemistry and Biology*; CRC Press: Boca Raton, FL, 1991: Vols. I and II.
(3) Weiss, R.; Gold, A.; Trautwein, A. X.; Ternier, J. In *The Porphyrin Handbook*; Kadish, K. M., Smith, K. M., Guilard, R., Eds.; Academic Press: NewYork, 2000; Vol. 4, p 65.
(4) Ortiz de Montellano, P. R., Ed. *Cytochrome P450: Structure, Mechanism and Biochemistry*; Plenum Press: New York, 1995.
(5) Meunier, B.; Robert, A.; Pratviel, G.; Bernadou, J. In *The Porphyrin Handbook*; Kadish, K. M., Smith, K. M., Guilard, R., Eds.; Academic Press: New York, 2000: Vol. 4, p 119.
(6) Maines, M. D. *Heme Oxygenase: Clinical Applications and Functions*; CRC Press: Boca Raton, FL, 1992
(7) Schmid, R.; McDonagh, A. F. In *The Porphyrins*; Dolphin, D., Ed.; Academic Press: New York, 1979; Vol. 6, p 258.
(8) Bissel, D. M. In *Liver: Normal Function and Disease*; Ostrow, J. D., Ed.; Marcel Decker, Inc.: New York, 1986; Vol. 4 (Bile Pigments and Jaundice), p 133.
(9) Ortiz de Montellano; P. R. *Acc. Chem. Res.* **1998**, *31*, 543.
(10) Verma, A.; Hirsch, D. J.; Glatt, G. E.; Ronnett, G. V.; Snyder, S. H. *Science* **1993**, *259*, 381.

10.1021/ja0016405 CCC: $19.00
Published on Web 11/23/2000

Scheme 2

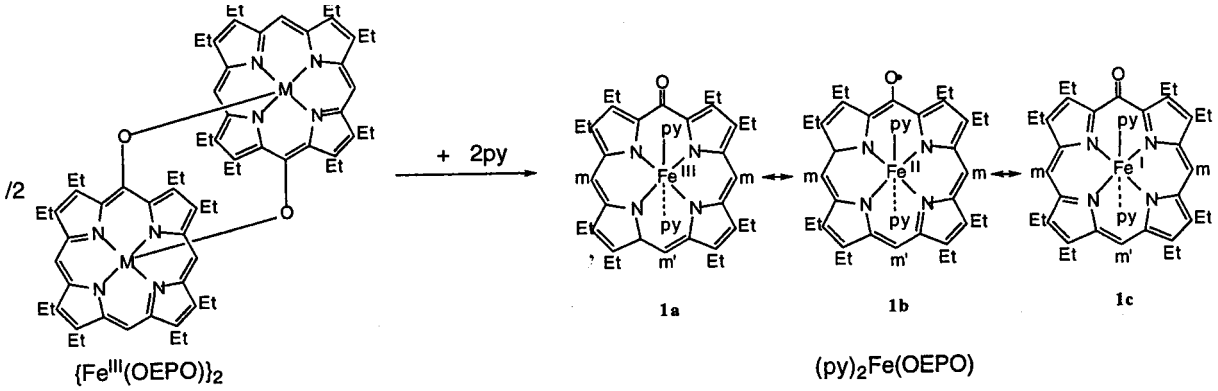

in the meso hydroxylation of the heme.[11−15] The major evidence for initial heme hydroxylation has come from studies that show that α-hydroxylated heme binds to heme oxygenase and can replace heme as a substrate for heme oxygenase. However, only recently has direct spectroscopic evidence been produced that suggests that a meso-hydroxylated heme is formed by heme oxygenase.[16]

The coupled oxidation process, in which heme degradation is brought about by dioxygen in the presence of a reducing agent (generally ascorbic acid), has been widely employed as a model for biological heme catabolism.[17−19] The coupled oxidation procedure can be utilized to oxidize iron porphyrins as model compounds[20,21] or to oxidize intact heme proteins. Coupled oxidation of heme alone produces a mixture of all four biliverdin isomers as a result of reaction at all four meso positions.[22] Moreover, the four isomers appear to be formed in nearly equal proportions, and the process does not show the regiospecificity displayed by heme oxygenase oxidation. However, with a trifluoromethyl-substituted heme, 7-demethyl-7-(trifluoromethyl)mesohemin IX, an unusually high degree of regiospecificity has been observed, and this specificity has been attributed to electronic control of the process.[23] Notably, coupled oxidation of myoglobin, as well as an active site variant of myoglobin, results in cleavage that occurs exclusively at the α-meso carbon.[24,25]

For coupled oxidation of $(py)_2Fe^{II}(OEP)$ in pyridine solution, meso hydroxylation produces $(py)_2$(FeOEPO), a compound in which the meso substituent is deprotonated.[19,26] This complex has received considerable study[27−30] and has recently been isolated in pure form in this laboratory.[31] $(py)_2$Fe(OEPO) is conveniently prepared by the addition of pyridine to the dimer, $\{Fe^{III}(OEPO)\}_2$,[32] in the absence of dioxygen as shown in Scheme 2.[33] While the crystallographic data on this species indicate that the iron is in a high-spin state, the assignment of the iron and ligand oxidation states in solutions of this complex is less clear, since it can be described by a combination of the three canonical structures shown as **1a**, **1b**, and **1c** in Scheme 2. Spectroscopically, $(py)_2$Fe(OEPO) is readily identified on the basis of its characteristic ^{1}H NMR spectrum which displays marked upfield shifts for the two types of meso protons and both upfield and downfield shifts for the methylene protons.

The regiospecificity of heme catabolism produced by heme oxygenase and by coupled oxidation of myoglobin has been ascribed to both steric and electronic factors.[34,35] The effect of meso-methyl versus meso-formyl substitution on the regiospecificity of HO reaction[36,37] and the NMR observation[38] of larger spin density at α-meso position in HO have led to the conclusion that electronic effects are important in regioselectivity. Recently, the crystal structure of human heme oxygenase-1 with the substrate (heme) bound has been reported.[39] The heme is sandwiched between two helical protein segments with the proximal helix providing histidine 25 as an axial ligand. There are two molecules of the heme/heme oxygenase complex in the asymmetric unit. One of these molecules offers more confinement of the heme with the distal helix restricting access to the

(11) Yoshida, T.; Noguchi, M.; Kikuchi, G.; Sano, S. *J. Biochem.* **1981**, *90*, 125.
(12) Sano, S.; Sano, T.; Morishima, I.; Shiro, Y.; Maeda, Y. *Proc. Natl. Acad. Sci. U.S.A.* **1986**, *83*, 531.
(13) Wilks, A.; Ortiz de Montellano, P. R. *J. Biol. Chem.* **1993**, *268*, 22357.
(14) Wilks, A.; Torpey, J.; Ortiz de Montellano, P. R. *J. Biol. Chem.* **1994**, *269*, 29553.
(15) Mansfield Matera, K.; Takahashi, S.; Fujii, H.; Zhou, H.; Ishikawa, K.; Yoshimura, T.; Rousseau, D. L.; Yoshida, T.; Ikeda-Saito, M. *J. Biol. Chem.* **1996**, *271*, 6618.
(16) Liu, Y.; Moënne-Loccoz, P.; Loehr, T. M.; Ortiz de Montellano, P. R. *J. Biol. Chem.* **1997**, *272*, 6909.
(17) Warburg, O.; Negelein, E. *Chem. Ber.* **1930**, *63*, 1816.
(18) Lagarias, J. C. *Biochim. Biophys. Acta* **1982**, *717*, 12.
(19) St Claire, T. N.; Balch, A. L. *Inorg. Chem.* **1999**, *38*, 684.
(20) Balch, A. L.; Latos-Grażyński, L.; Noll, B. C.; Olmstead, M. M.; Szterenberg, L.; Safari, N. *J. Am. Chem. Soc.* **1993**, *115*, 1422.
(21) Balch, A. L.; Latos-Grażyński, L.; Noll, B. C.; Olmstead, M. M.; Safari, N. *J. Am. Chem. Soc.* **1993**, *115*, 9056.
(22) Bonnett, R.; McDonagh, A. F. *J. Chem. Soc., Perkin Trans. 1* **1973**, 881.
(23) Crusats, J.; Suzuki, A.; Mizutani, T.; Ogoshi, H., *J. Org. Chem.* **1998**, *63*, 602.
(24) O'Carra, P.; Colleran, E. *FEBS Lett.* **1969**, *5*, 295.
(25) Hildebrand, D. P.; Tang, H.; Luo, Y.; Hunter, C. L.; Smith, M.; Brayer, G. D.; Mauk, A. G. *J. Am. Chem. Soc.* **1996**, *118*, 12909.
(26) Balch, A. L. *Coord. Chem. Rev.* **2000**, *200−202*, 349.
(27) Sano, S.; Sugiura, Y.; Maeda, Y.; Ogawa, S.; Morishima, I. *J. Am. Chem. Soc.* **1981**, *103*, 2888.
(28) Morishima, I.; Fujii, H.; Shiro, Y. *J. Am. Chem. Soc.* **1986**, *108*, 3858.
(29) Morishima, I.; Shiro, Y.; Hiroshi, F. *Inorg. Chem.* **1995**, *34*, 1528.
(30) Balch, A. L.; Noll, B. C.; Reid, S. M.; Zovinka, E. P. *Inorg. Chem.* **1993**, *32*, 2610.
(31) Balch, A. L.; Koerner, R.; Latos-Grażyński, L.; Noll, B. C. *J. Am. Chem. Soc.* **1996**, *118*, 2760.
(32) Balch, A. L.; Latos-Grażyński; Noll, B. C.; Olmstead, M. M.; Zovinka, E. P. *Inorg. Chem.* **1992**, *31*, 2248.
(33) Balch, A. L.; Noll, B. C.; Reid, S. M.; Zovinka, E. P. *Inorg. Chem.* **1993**, *32*, 2610.
(34) O'Carra, P. In *Porphyrins and Metalloporphyrins*; Smith, K. M., Ed.; Elsevier Scientific Pub. Co.: New York, 1975; p 123.
(35) Brown, S. B.; Chabot, A. A.; Enderby E. A.; North A. C. T. *Nature* **1981**, *289*, 93.
(36) Torpey, J.; Ortiz de Montellano, P. R., *J. Biol. Chem.*, **1996**, *271*, 26067.
(37) Torpey, J.; Ortiz de Montellano, P. R., *J. Biol. Chem.*, **1997**, *272*, 22008.
(38) Hernández, G.; Wilks, A.; Paolesse, R.; Smith K. M.; Ortiz de Montellano, P. R.; La Mar, G. N. *Biochemistry* **1994**, *33*, 6631.
(39) Schuller, D.; Wilks, A.; Ortiz de Montellano, P. R.; Poulos T. *Nature Struct. Biol.* **1999**, *6*, 861.

Scheme 3

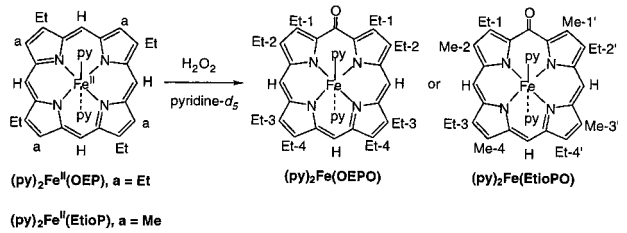

β-, γ-, and δ-meso carbon atoms while the other molecule provides less steric constraint with both the α- and δ-meso carbon atoms accessible to attack. There are no specific basic or acidic residues in proximity to the α-meso carbon to participate in the meso hydroxylation step. While the crystal structure does support the notion of steric control of the regiochemistry of the initial hydroxylation, electronic factors may also play a role in directing this step, especially with non-natural heme substrates. Additionally, recent ^{1}H NMR studies have revealed that a new species can be detected soon after substrate binding and it appears that heme seating within HO may be subject to dynamic effects that complicate the structural picture and the role of steric effects in determining regioselectivity.[40]

Previously, Bonnett and Dimsdale were able to isolate metal-free octaethyloxophlorin in low yield from the reaction of hydrogen peroxide with $(py)_2Fe^{II}$(OEP) and reported that an olive-green intermediate was formed.[41] Here, we report observations regarding the direct oxidation of hemes by hydrogen peroxide in pyridine solution in the absence of dioxygen or of a reducing agent. Thus, these reactions differ significantly from previous work on heme degradation that utilizes dioxygen with heme oxygenase or coupled oxidation conditions. By monitoring the reaction directly by ^{1}H NMR spectroscopy, the regiospecificity of the initial heme modification process can be examined without the problems inherent in separation and isolation of products.

Results and Discussion

^{1}H NMR Investigations of the Reaction of Hydrogen Peroxide with Symmetrical Iron Porphyrins, $(py)_2Fe^{II}$(OEP) and $(py)_2Fe^{II}$(EtioP). To characterize the species formed during the reactions of iron(II) porphyrins with hydrogen peroxide, we have examined the reactions of the symmetric iron porphyrins, $(py)_2Fe^{II}$(OEP) and $(py)_2Fe^{II}$(EtioP), with hydrogen peroxide at −30 °C in the absence of dioxygen. Scheme 3 shows the structures and transformations involved. Pyridine-d_5 solutions of these complexes were prepared under a dinitrogen atmosphere to exclude any oxidation by dioxygen and cooled to −30 °C, at which point a dioxygen-free hydrogen peroxide (50% in water)/pyridine-d_5 solution (1:60 v/v) was introduced into the sample. The red solutions of the Fe^{II} porphyrins turned brownish green upon addition of the hydrogen peroxide, and the ^{1}H NMR spectra showed the presence of new sets of resonances due to the conversion of the low-spin, diamagnetic starting materials into new, paramagnetic products. After reaction, there was no evidence for the formation of any precipitate, and so the spectral data are indicative of the entire course of the reaction. Once formed at −30 °C, the resulting samples are stable as long as they are protected from dioxygen. Relevant ^{1}H NMR spectra obtained at 20 °C are shown in Figure 1.

(40) Yeh, S.; La Mar, G. N.; Wilks, A.; Ortiz de Montellano, P. R., personal communication.

(41) Bonnett, R.; Dimsdale, M. J. *J. Chem. Soc., Perkin Trans 1* **1972**, 2540.

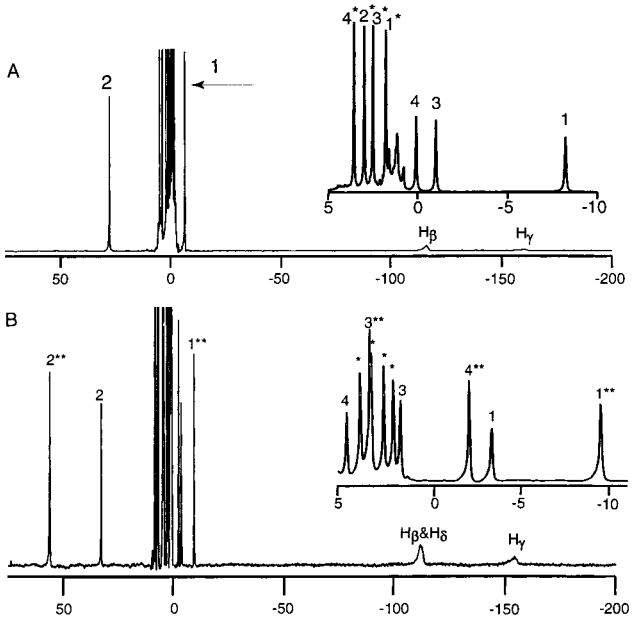

Figure 1. 500-MHz ^{1}H NMR spectra taken at 20 °C from the reaction of $(py)_2Fe^{II}$(OEP) (trace A) and $(py)_2Fe^{II}$(EtioP) (trace B) in pyridine-d_5 with hydrogen peroxide added at −30 °C with subsequent warming to 20 °C. The inset to trace A was recorded at −30 °C to obtain the best resolution. Methylene resonances are designated by 1−4, methyl resonances of ethyl groups are designated by 1*−4*, and pyrrole methyl resonanes are designated by 1**−4**. In trace B, the methyl resonances of the ethyl groups are indicated by *.

Scheme 4

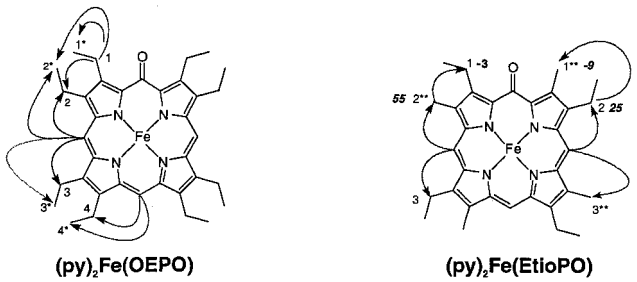

The results of oxidation of $(py)_2Fe^{II}$(OEP) are shown in trace A. The characteristic resonances of $(py)_2$Fe(OEPO) are clearly observed with two meso resonances in a 2:1 intensity ratio with marked upfield hyperfine shifts and with two of the four methylene resonances observed outside of the diamagnetic region (0−10 ppm).[27] The other resonances (two methylene resonances, four methyl resonances) of $(py)_2$Fe(OEPO) are observed in the −5 to +10 ppm region of the spectrum as seen in the inset to trace A. Note that no other resonances are present and consequently the reaction proceeds cleanly without the formation of other potential paramagnetic oxidation products: $[(py)_2Fe^{III}(OEP)]^+$, $(py)Fe^{IV}$=O(OEP), or $(OEP)Fe^{III}OFe^{III}$(OEP).

A complete assignment of the spectrum of $(py)_2$Fe(OEPO) has been made through the use of 1D NOE difference spectra. The data are presented in Figure S1 in the Supporting Information. The pattern of connectivity obtained from the NOE difference peaks is set out in Scheme 4. Irradiation of the far upfield meso resonance (H_γ) produces difference NOE peaks corresponding only to resonances 4 and 4* in trace A of Figure 1. Hence, methyl resonance 4* and methylene resonance 4 originate from the ethyl group protons in positions Et-4 in the structure of $(py)_2$Fe(OEPO) shown in Scheme 3. Irradiation of the other meso resonance (H_β) produces difference NOE peaks

corresponding to methylene resonances 2 and 3 and methyl resonances 2* and 3*. Hence, these resonances belong to the ethyl protons of positions Et-2 and Et-3 that flank H_β (see Scheme 3). Irradiation of the downfield methylene resonance (2) produces a strong NOE difference peak corresponding to methyl resonance 2* and weaker peaks to resonances 1 and 1*. These data allow us to assign resonances 2 and 2* to the ethyl groups in position Et-2 in Scheme 3, resonances 1 and 1* to the ethyl groups in position Et-1 in the same diagram, and resonances 3 and 3* to the ethyl groups in position Et-3.

Trace B of Figure 1 shows the ^{1}H NMR spectrum that results from treatment of $(py)_2Fe^{II}$(EtioP) with hydrogen peroxide. The spectral pattern is consistent with the formation of $(py)_2$Fe(EtioPO). The resonances of $(py)_2$Fe(EtioPO) are readily assigned through their relative intensities and comparison with the spectrum of $(py)_2$Fe(OEPO), which is shown in trace A. Thus, the ^{1}H NMR spectrum of $(py)_2$Fe(EtioPO) contains four new resonances that are not observed in the spectrum of $(py)_2$Fe(OEPO). These four new resonances, which are observed at 55, 3, −2, and −9 ppm, are assigned to the four pyrrole methyl groups in $(py)_2$Fe(EtioPO). As usual for heme systems, pyrrole-bound methyl groups display greater hyperfine shifts than do the corresponding pyrrole-bound methylene groups,[42,43] and the methyl and methylene resonances can be grouped in pairwise fashion: methyl at 55 with methylene at 25 ppm, methyl at −9 with methylene at −3 ppm, methyl at −2 with methylene at 4.5 ppm, and methyl at 3 with methylene at 2 ppm. Otherwise the spectrum of $(py)_2$Fe(EtioPO) contains all of the resonances found for $(py)_2$Fe(OEPO), and all of these resonances have hyperfine shifts that are nearly identical to those found for $(py)_2$Fe(OEPO). Consequently, the substitution of methyl groups for ethyl groups does not produce a major perturbation of the electronic structure and spin distribution within the complex. The characteristic resonances of the meso protons of $(py)_2$Fe(EtioPO) are observed with marked upfield hyperfine shifts, although the differences between symmetry-inequivalent β- and δ-meso resonances are not resolved.

Further assignments of the spectrum of $(py)_2$Fe(EtioPO) have been obtained from 1D NOE difference spectra. Relevant data are given in Figure S2 of the Supporting Information, and the connectivity pattern is set out in Scheme 4. Irradiation of the downfield meso resonance that originates from the protons (H_β and H_δ) produces NOE difference peaks that correspond to the resonances labeled 2, 2**, 3, and 3** in trace B of Figure 1. Hence, these resonances must originate from the groups in positions Me-2, Et-2′, Et-3, and Me-3′ in the structure of $(py)_2$Fe(EtioPO) given in Scheme 3. Irradiation of the methyl resonance at 55 ppm (resonance 2**) results in an NOE difference peak corresponding to the methylene resonance at

Scheme 5

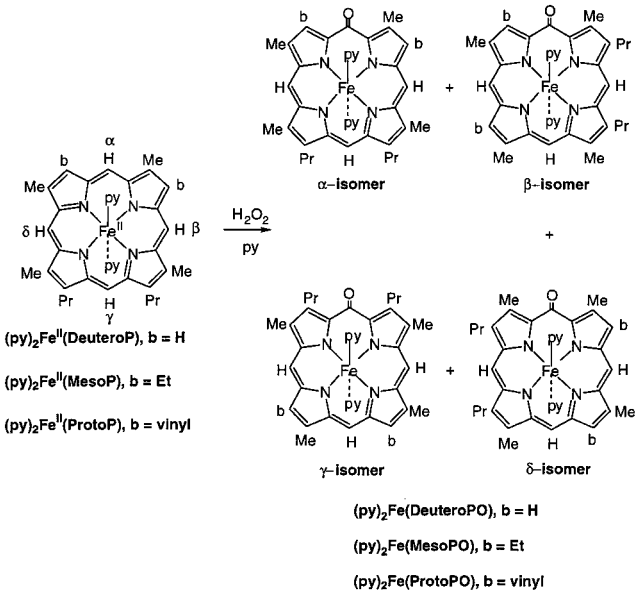

−3 ppm (resonance 1). This is consistent with assigning resonance 2** to methyl group Me-2 and resonance 1 to the methylene group of Et-1. Irradiation of the methylene resonance at 25 ppm (resonance 2) results in a NOE difference peak at −9 ppm (resonance 1**). This is consistent with assigning resonance 2 to the methylene group of ethyl group Et-2′ and resonance 1** to the methyl group Me-1′. Thus, resonances 3 and 3**, which have NOE difference peaks that connect them to H_β and H_δ, must originate in Me-3′ and Et-3. The remaining resonances, 4 and 4′, can then be assigned to Me-4 and to the methylene resonances of Et-4′. This set of assignments is also completely in accord with the assignments made for $(py)_2$Fe(OEPO).

Reaction of Hydrogen Peroxide with Unsymmetrical Iron Porphyrins. (1) Spectroscopic Results. The reactions of the unsymmetrical hemes, $(py)_2Fe^{II}$(DeuteroP) and $(py)_2Fe^{II}$(MesoP), and $(py)_2Fe^{II}$(ProtoP), which are shown in Scheme 5, with hydrogen peroxide have been examined under the conditions used for the reaction of hydrogen peroxide with $(py)_2Fe^{II}$(OEP) and $(py)_2Fe^{II}$(EtioP).

Figure 2 shows spectra for each of these unsymmetrical hemes in the upfield region where the meso resonances are expected to occur. The spectrum obtained by oxidation of $(py)_2Fe^{II}$(DeuteroP) with hydrogen peroxide is shown at 20 °C in trace A. This temperature gives the best resolution of all of the resonances observed. The corresponding spectra obtained by treating $(py)_2Fe^{II}$(MesoP) and $(py)_2Fe^{II}$(ProtoP) with hydrogen peroxide are shown in traces B and C of Figure 2. These spectra were recorded at −30 °C where again the resolution is best. In each case, the overall pattern of resonances is similar to that seen for $(py)_2$Fe(OEPO) in the upfield region of Figure 1. However, it is also abundantly clear that multiple resonances are present in each of the three traces in Figure 2. Consequently, several different species are formed upon oxidation. Unfortunately, the resolution within this region of each spectrum is not sufficient to allow a thorough analysis of the species present. Examination of the most upfield region in trace A, where the resolution of the meso resonances is best, does show that three individual meso resonances are present and that these have unequal intensities. Comparison with the data given in Figure 1 allows these resonances to be assigned to the single meso protons opposite to the oxygenated site in the porphyrin. Thus,

(42) If the spin density at the β-pyrrole carbon positions is identical, π-contact shifted pyrrole-bound methyl groups display greater hyperfine shifts than do the corresponding pyrrole-bound methylene group. Theoretically, the contact shift of the individual CH proton is proportional to $A_{CH_2R} = Q_{CH_2R}\rho/2S = (B_0 + B_2\cos^2\theta\rho/2S)$, where Q_{CH_2R}, K, B_o, and B_2 are constants and ρ is π-spin density at a carbon atom.[43, 44] Typically B_0 is very small; thus, $A_{CH_2R} = Q_{CH_2R}\rho/2S = B_2\cos^2\theta\rho/2S$. The orientation of the CH proton is conveniently described by a dihedral angle θ between the plane determined by the p_z axis of the β-pyrrole carbon (C_β) and the C_β−C_{methyl} bond and the C_β−C_{methyl}−H bonds. For the methyl group rotating between three positions of the idealized geometry (θ = 0, 120, 240), the averaged contact shift will be proportional to $0.5(B_2\rho K/2S)$. Once the β-methyl group is replaced by the ethyl group, the bulky methyl fragment of the β-ethyl group tends to be located furthest away from the porphyrin plane ($\theta = 0°$). Thus, this arrangement sets the lowest limit for the estimated shift of the methylene resonances as equal to $0.25(B_2\rho K/2S)$.

(43) Pignolet, L. H.; La Mar, G. N. In *NMR of Paramagnetic Molecules*; La Mar, G. N., Horrocks, W. D., Jr., Holm, R. H., Eds.; Academic Press: New York, 1973; p 357.

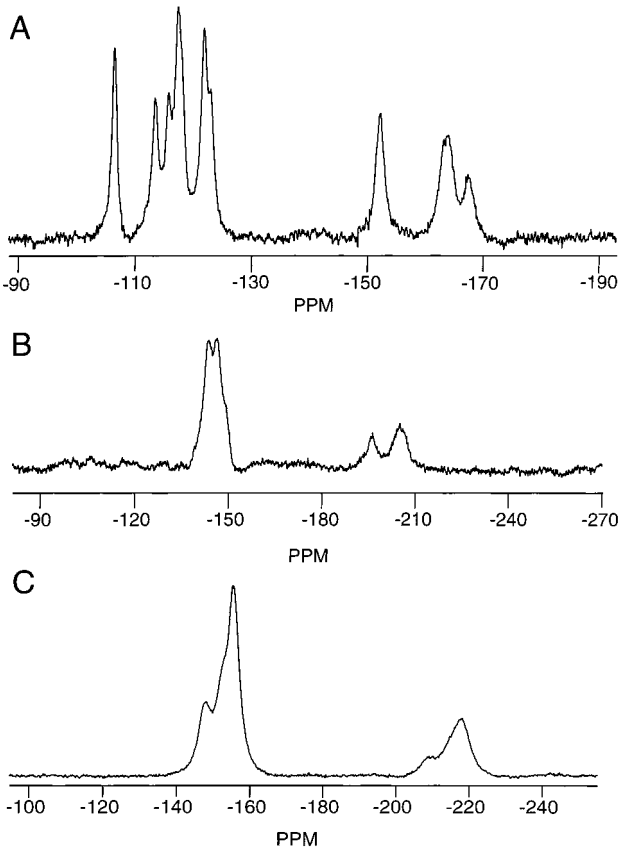

Figure 2. Far-upfield region of the 500-MHz ^{1}H NMR spectra from the reaction of (A) $(py)_2Fe^{II}$(DeuteroP), (B) $(py)_2Fe^{II}$(MesoP), and (C) $(py)_2Fe^{II}$(ProtoP) with hydrogen peroxide (added at −30 °C) in pyridine-d_5 at −30 °C. The spectrum in trace A was recorded with the sample at 20 °C, while the spectra in traces B and C were obtained from samples at −30 °C.

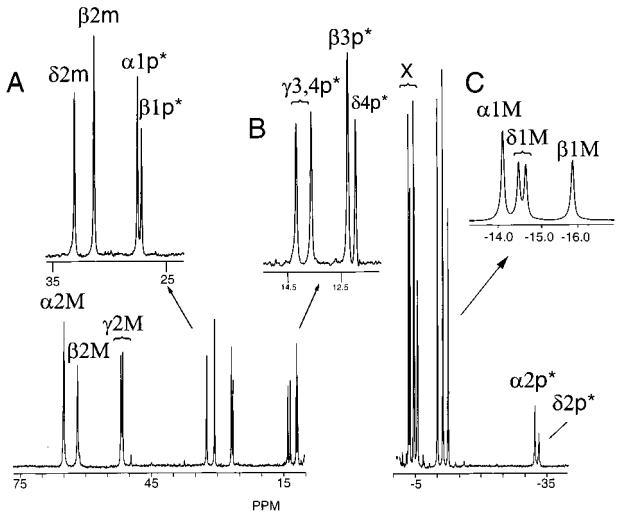

Figure 3. Portions of the 500-MHz ^{1}H NMR spectrum recorded at 20 °C from the reaction of $(py)_2Fe^{II}$(DeuteroP) in pyridine-d_5 with hydrogen peroxide added at −30 °C and subsequently warmed to 20 °C. Inset A shows an expansion of the 35−25 ppm region (propionate methylene resonances) at 20 °C, inset B shows an expansion of the 14.5−12.5 ppm region at 20 °C, and inset C shows an expansion of the −14 to −16 ppm region at 0 °C. Resonances are identified by three characters The first character indicates the isomer (α, β, γ, or δ) that produces the resonance. The second character identifies the position site (1, 2, 3, or 4) of the functional group (see Scheme 5). The final character specifies the chemical nature of the functional group, M methyl-H, m, methylene-H, or p, pyrrole-H.

at least three of the four possible isomeric complexes shown in Scheme 4 are present in the sample of $(py)_2$Fe(DeuteroPO) and their abundances are unequal.

The 75 to −40 ppm region of the ^{1}H NMR spectra obtained by reaction of $(py)_2Fe^{II}$(DeuteroP), $(py)_2Fe^{II}$(MesoP), and $(py)_2Fe^{II}$(ProtoP) with hydrogen peroxide are shown in Figures 3−5, respectively. These spectra are shown at the temperatures at which each has the best resolution. The various insets show additional details of particular features. In some cases, these insets were recorded at a different temperature where that particular feature shows enhanced resolution. Assignments of the individual resonances to the possible isomeric products are also made. The procedure used to identify the resonances and assign them to specific isomers is given in the next section.

(2) Analysis of the ^{1}H NMR Spectra and Assignment of Resonances to Specific Isomeric Products. General Considerations. Two issues need to be addressed in interpreting the spectra shown in Figures 2−5. Resonances need to be assigned to specific functional groups within each product, and they also need to be assigned to individual isomers, where possible. The data shown in Figure 1 for the symmetrical hemes allows certain regions of the ^{1}H NMR spectra shown in Figures 2−5 to be associated with particular functional groups. Thus, all of the resonances seen in Figure 2 are assigned to meso protons, and those resonances with the most negative chemical shifts are assigned to the meso protons opposite the site of oxygenation. In Figures 3−5, the most downfield resonances, those with chemical shifts greater than 45 ppm, are assigned to a pyrrole methyl group and will be termed the downfield methyl resonances. Resonances in the 25−30 ppm region (downfield methylene region) are assigned to the protons of pyrrole-bound methylene groups. Resonances in the −10 to −20 ppm region are similarly assigned to another pyrrole methyl group. This region will be referred to as the upfield methyl region. Resonances in the 0 to −10 ppm region are assigned to remaining pyrrole-bound methylene and methyl groups.

To assign resonances to individual isomers, we proceed under the proposition that the pattern of the spin density distribution is dominated by the location of the oxygenated meso site and that this functional group imposes a basic 2-fold electronic symmetry on the porphyrin (as shown in structure 1 in Scheme 6) which is only moderately perturbed by the presence of other functional groups. Thus, the unpaired spin densities at the pairs of positions, 1 and 1′, are expected to be similar. Additionally, the spin densities at positions 2 and 2′ are also anticipated to be similar, and so on. Thus, the δ-isomer, which has two methyl groups at positions 1 and 1′, is expected to exhibit two equally intense resonances with very similar chemical shifts for these methyl protons. Likewise, the γ-isomer, with methyl groups in the positions 2 and 2′, is expected to display a pair of equally intense resonances with similar chemical shifts for these methyl groups.

The published spectrum[12] of the individual α-isomer of $(py)_2$Fe(ProtoPO) allows certain key features of all of the spectra to be understood and facilitates the interpretation of the data shown in Figure 5. For our assignment purposes, the most significant features in the spectrum of the α-isomer of $(py)_2$Fe-(ProtoPO) are the single, widely dispersed methyl resonances at 46 and −12 ppm which are differentiated by the sign of the isotropic shifts. These resonances must arise from methyl groups on the A and A′ pyrrole rings (positions 1 and 2). The two methyl groups on pyrrole rings B and B′ in positions 3 and 3′ should produce a pair of resonances with identical sign and similar values for the hyperfine shifts. (There are no methyl

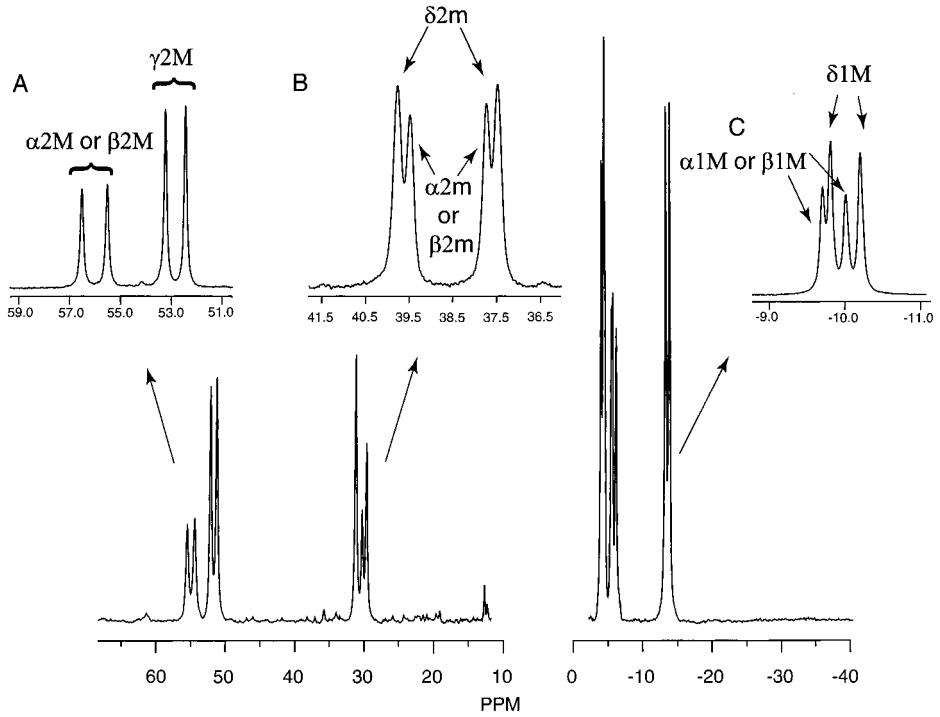

Figure 4. Portions of the 500-MHz ^{1}H NMR spectrum taken at −30 °C from the reaction of $(py)_2Fe^{II}$(MesoP) in pyridine-d_5 with hydrogen peroxide (added at −30 °C). Inset A shows an expansion of the 59−51 ppm region (pyrrole methyl resonances) at 20 °C, inset B shows an expansion of the 41−36.5 ppm region (propionate methylene resonances) at 60 °C, and inset C shows an expansion of the −9 to −11 ppm region (propionate methylene resonances) at 20 °C. Resonance assignments follow those used in Figure 3.

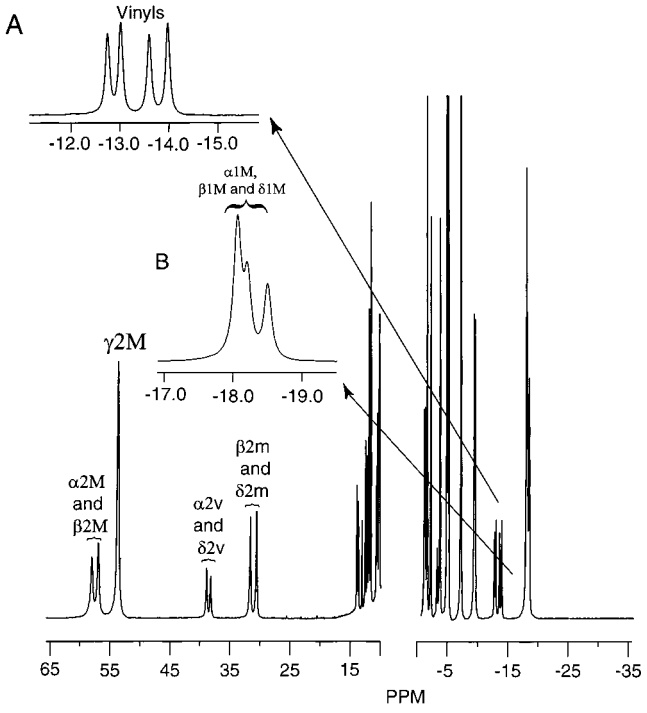

Figure 5. Portions of the 500-MHz ^{1}H NMR spectra obtained from the reaction of $(py)_2Fe^{II}$(ProtoP) in pyridine-d_5 with hydrogen peroxide at −30 °C. Inset A shows an expansion of the −12 to −15 ppm region (vinyl resonances) at −30 °C, and inset B shows an expansion of the −17 to −19 ppm region (propionate methylene resonances). All data were obtained with the sample at −30 °C. Resonance assignments follow those used in Figure 3 but with v indicating resonances arising from heme vinyl protons.

groups in positions 4 and 4′.) Since the resonances observed at 46 and −12 ppm are single lines with opposite signs for the hyperfine shifts, they cannot come from the methyl groups in

Scheme 6

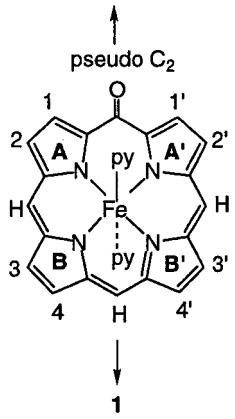

positions 3 and 3′, which would have to produce a doublet with the same sign for the hyperfine shifts. Consequently, in the spectra shown in Figures 3−5, the methyl resonances in the downfield methyl region (chemical shift greater than 45 ppm) and in the upfield methyl region at −10 to −20 ppm are assigned to methyl groups on pyrrole rings A and A′ in each isomer.

This set of considerations is also entirely consistent with the assignment of resonances in the spectra of $(py)_2$Fe(OEPO) and $(py)_2$Fe(EtioPO) that have been obtained using NOE difference spectra. Specifically for $(py)_2$Fe(EtioPO), the downfield methyl resonance has been assigned to Me-2 and the upfield methyl resonance to Me-1′ and these functional groups are on pyrrole rings A and A′, respectively.

For $(py)_2Fe^{II}$(DeuteroP). Portions of the ^{1}H NMR spectrum obtained by treatment of $(py)_2Fe^{II}$(DeuteroP) with hydrogen peroxide are shown in Figures 2 and 3. Resonance assignments have been greatly assisted by comparison of the data shown in Figure 3 with data obtained from a sample of $(py)_2Fe^{II}$-

(DeuteroP), which was specifically deuterated in the two pyrrole C−H positions. That sample lacked the resonances indicated by an asterisk in Figure 3. (Also these pyrrole C−H resonances are absent from the spectrum obtained from a sample of $(py)_2Fe^{II}$(MesoP) that was treated with hydrogen peroxide; see Figure 4.) There are eight pyrrole C−H resonances seen in the spectra shown in Figure 3. (Two of these resonances have upfield chemical shifts and these resonances will be described as lying within the upfield pyrrole-H region.) Hence, all four isomers of $(py)_2$Fe(DeuteroPO) are present and all eight of the expected pyrrole C−H resonances are observed. However, the variation in intensities of these eight resonances indicates that the four isomers are present in a nonrandom population. This is a very important piece of information because of its analytical applications. Careful comparison of the relative intensities allows the selection of four pairs of resonances, which belong to the four regioisomers shown in Scheme 4. The internal consistency of the integrated intensities for each set has been carefully checked. Resonances that belong to one isomer have a set of relative intensities that reflect the molecular structure. However, the intensity ratios between resonances that belong to different isomers reflect the relative populations of those isomers as determined by the regiospecificity of the reaction. Since the four isomers are present in a nonrandom population, these considerations are efficient in identifying the resonances of individual isomers.

Substitution of a methyl group by a proton is expected to give rise to a resonance that is subject to a hyperfine shift of opposite sign but a magnitude comparable to that of the corresponding methyl group if π-spin delocalization dominates the hyperfine shifts.[44] Consequently, the resonances in Figure 3 with the largest hyperfine shifts, those in the downfield methyl region and those in the upfield pyrrole C−H region, must originate from a common site (i.e., from a site with similar value and sign of the spin density) within the product molecule. Likewise, when methylene groups and methyl groups occupy analogous sites, these groups will produce resonances with hyperfine shifts of the same sign but the magnitude of the hyperfine shift of the methyl group will be greater. Consequently, the resonances in the downfield methyl region, the downfield methylene region, and the upfield pyrrole-H region must arise from substituents in either the 1 and 1′ or in the 2 and 2′ positions on pyrrole rings A and A′ in Scheme 5.

If the resonances in these regions are produced by protons in the 1 and 1′ positions, then the γ-isomer will produce a doublet with equally intense resonances in the downfield methylene region. No other isomer will produce a doublet methylene resonance in this region. Inspection of this region of the spectrum shows two resonances with clearly unequal intensity; consequently, this assignment is untenable. On the other hand, if the resonances in the downfield methyl region and the upfield pyrrole-H region come from groups in the 2 and 2′ positions, then two unequally intense resonances are excepted in the downfield methylene region. These resonances arise from the single methylene group in the β (2′-CH_2)- and in the δ (2-CH_2) -isomers. The α- and γ-isomers do not have methylene groups in the 2 and 2′ positions and hence cannot contribute to this region of the spectrum. Indeed, two unequally intense methylene resonances are observed in this region (see inset A in Figure 3). Consequently, the resonances in the downfield methyl region, the downfield methylene region, and the upfield pyrrole-H region are assigned to positions 2 and 2′,

(44) Walker, A. In *The Porphyrin Handbook*; Kadish, K. M., Smith, K. M., Guilard, R., Eds.; Academic Press: New York, 2000; Vol. 5, p 82.

Table 1. Distribution of Isomers in Pyridine-d_5

heme	α	*β*	*γ*	*δ*
$(py)_2$Fe(DeuteroPO)	31	24	25	20
$(py)_2$Fe(MesoPO)	18	18	36	28
$(py)_2$Fe(ProtoPO)	20	22	35	23
nonselective	25	25	25	25

the resonances in the region at −10 to −20 ppm arise from methyl substituents in the 1 and 1′ positions, and resonances in the 25−30 ppm region arise from pyrrole protons in the 1 and 1′ positions.

Following the above analysis, it is possible to assign individual resonances in Figure 3. The following three-character scheme is used. The first character indicates which isomer, α, *β*, *γ*, or *δ*, produces the resonance. The second character identifies the position (site 1, 2, 3, or 4 as in Scheme 5). We do not differentiate between 1 and 1′, etc., of the functional group within the product. The final character specifies the chemical nature of the functional group: M, methyl-H; m, methylene-H; and p, pyrrole-H (v, vinyl-H). Thus, the most downfield resonance in the spectrum shown in Figure 3 is labeled α2M, indicating that it arises from a methyl group in the 2 or 2′ position in the α-isomer of $(py)_2$Fe(DeuteroPO).

Four resonances appear in the downfield methyl region. Two have identical intensity and hence are due to the *γ* isomer, which has two methyl groups in the 2 and 2′ positions, The other two resonances are due to the α- and *β*-isomers. In the upfield methyl region between −5 and −20 ppm, there are also four resonances, a pair with equal intensity, which come from the *δ*-isomer, and two resonances whose intensities parallel those seen in the downfield methyl region. The resonances can be assigned to the α- and *β*-isomers, and they can be paired with partners in the downfield methyl region on the basis of their relative integrated intensities.

The resonances of the α- and, by default, the *β*-isomers, have also been differentiated by comparison of the intensities of the downfield (∼27 ppm) and upfield (∼−34 ppm) shifted pyrrole resonances. This analysis selected two pyrrole resonances (of equal intensity but opposite hyperfine shifts) which must belong to the α-isomer. Once these resonances are identified, they serve as a convenient starting point for the identification of the other resonances of the α-isomer through analysis of the relative integrated intensities of other resonances.

Further analysis of the integrated intensities of the resonances in the spectra obtained from $(py)_2Fe^{II}$(DeuteroP) indicates that the four isomers shown in Scheme 4 are formed in the following percentages: α, 31; *β*, 24; *γ*, 25; and *δ*, 20. Table 1 shows these percentages in a format that facilitates comparison with the corresponding percentages obtained from the reaction of $(py)_2Fe^{II}$(MesoP) and $(py)_2Fe^{II}$(ProtoP) with hydrogen peroxide.

Attempts to utilize NOE difference spectra to obtain additional confirmatory assignments of this spectrum have not been successful. The inability to detect NOE difference peaks is caused by two factors: the low symmetry of each isomer and the fact that four different isomers are produced. As a result, the spectral intensity is lower and the cross-peaks are too weak to detect. We were unable to improve the signal intensity by increasing solute concentration due to the need to keep all species in solution during the reaction at −30 °C.

To examine this reaction at lower temperatures where intermediates might be detected, the reactions of hydrogen peroxide with $(py)_2Fe^{II}$(DeuteroP) were examined in mixtures of dichloromethane and pyridine. Although working at low temperature in this solvent mixture did not reveal the presence

Table 2. Distribution of Isomers for $(py)_2Fe$(DeuteroPO) in Different Solvent Mixtures

solvent	α	β	γ	δ
pure pyridine-d_5	31	24	25	20
pyridine-d_5/dichloromethane−d_2 (9:1)	19	14	40	27
pyridine-d_5/dichloromethane−d_2 (1:1)	21	13	39	27
pyridine-d_5/dichloromethane−d_2 (1:5)	28	22	29	21
nonselective	25	25	25	25

of any new intermediates, these studies did reveal that the regioselectivity of this oxidation is solvent dependent. As seen in Table 2, the relative proportions of the four isomers formed changes as the solvent composition is altered.

For $(py)_2Fe^{II}$(MesoP). ^{1}H NMR spectra obtained from samples prepared by treatment of $(py)_2Fe^{II}$(MesoP) with hydrogen peroxide are shown in Figures 2 and 4. As expected, the spectra of $(py)_2Fe$(MesPO) lack the eight pyrrole C−H resonances seen in Figure 3 for $(py)_2Fe$(DeuteroPO). The resonance assignments shown in Figure 4 have been made by utilizing the information obtained and analyzed in the preceding sections.

For oxidation of $(py)_2Fe^{II}$(MesoP) in pyridine solution, the four isomers of $(py)_2Fe$(MesoPO) shown in Scheme 4 are formed in the percentages shown in Table 1.

For $(py)_2Fe^{II}$(ProtoP). Portions of the ^{1}H NMR spectra of $(py)_2Fe$(ProtoPO), which was obtained by hydrogen peroxide oxidation of a pyridine-d_5 solution of $(py)_2Fe^{II}$(ProtoP), are shown in Figures 2 and 5. Spectral analysis follows the course outlined above. A set of resonances that are not present in the spectra shown in Figures 3 and 4 are assigned to the protons of the vinyl groups in $(py)_2Fe$(ProtoPO). In Figure 5, these vinyl resonances are denoted by a v in the three character designation.

Reaction of $(py)_2Fe^{II}$(ProtoP) with hydrogen peroxide produces all four isomers of $(py)_2Fe$(ProtoPO) in the percentages shown in Table 1.

Conclusions

The results reported here demonstrate that hydrogen peroxide reacts cleanly with iron(II) porphyrins in pyridine solution under an inert atmosphere to form the corresponding oxophlorin complexes, which are stable in the absence of dioxygen. This process mimics the initial stage of heme degradation that is catalyzed by heme oxygenase. It is important to note that the process described here is distinct from the process of coupled oxidation in which a heme or heme protein is treated with dioxygen in the presence of a sacrificial reducing agent, which is generally either ascorbic acid or a hydrazine such as phenyl hydrazine.[19]

The general similarity in the ^{1}H NMR spectral patterns seen for all of the complexes produced here, $(py)_2Fe$(OEPO), $(py)_2Fe$(EtioPO), $(py)_2Fe$(DeuteroPO), $(py)_2Fe$(MesoPO), and $(py)_2Fe$(ProtoPO), indicates that all of these complexes have similar electronic structures. Consequently, all of these complexes need the set of resonance structures shown in Scheme 2 to describe the possible distribution of electrons between the ligands and iron center.

No evidence for the formation of intermediates in the process of conversion of $(py)_2Fe^{II}$(P) into $(py)_2Fe$(PO) through the reaction with hydrogen peroxide has been found. Other potential paramagnetic oxidation products, the one-electron oxidation product $[(py)_2Fe^{III}(OEP)]^+$, the ferryl complex $(py)Fe^{IV}$═O(OEP), or the ubiquitous μ-oxo dimer $(OEP)Fe^{III}OFe^{III}(OEP)$, which could have formed, are not detected in these experiments. Thus, aspects of the mechanism for this hydroxylation remain open to consideration. However, the present results are consistent with the notion that a heme-bound peroxide ligand may be involved in the attack upon the meso sites within the porphyrin.[9]

In contrast to the results reported here, addition of hydrogen peroxide to the heme proteins, myoglobin and horseradish peroxidase, results in the formation of ferryl, $(Fe{=}O)^{2+}$, forms of these proteins.[45,46] In these proteins, the iron is present in five-coordinate form that may facilitate coordination of the peroxide and its eventual cleavage to produce the ferryl complex. However, the reaction of the heme/heme oxygenase complex, which also contains a five-coordinated heme, with hydrogen peroxide does not produce an observable ferryl form; rather, the heme is converted by hydrogen peroxide into verdoheme.[13] However, a ferryl complex is formed by the reaction of the heme/heme oxygenase complex with *m*-chloroperoxybenzoic acid or *tert*-butyl hydroperoxide.[13] Although spectroscopically detectable amounts of ferryl hemes can be obtained at low temperatures by reacting iron porphyrins under carefully controlled conditions with dioxygen,[47] iodosyl benzene,[48] or *m*-chloroperoxybenzoic acid, we are not aware of any experiments where the reaction of hydrogen peroxide with a iron porphyrin complex results in the formation of a spectroscopically detected ferryl compound.[49]

The spectra obtained from oxidation of the unsymmetrically substituted hemes, $(py)_2Fe^{II}$(DeuteroP), $(py)_2Fe^{II}$(MesoP), and $(py)_2Fe^{II}$(ProtoP), indicate that the four isomeric oxophlorin products are formed in arrays that are somewhat nonselective but do not show a pronounced regiospecificity. Only in the case of oxygenation of $(py)_2Fe^{II}$(DeuteroP) in pyridine-d_5 solution is the α-isomer of the iron oxophlorin the major isomer that is produced, and the specificity is small. For the other two hemes studied, $(py)_2Fe^{II}$(MesoP) and $(py)_2Fe^{II}$(ProtoP), the γ-isomer is the most abundant and the α-isomer is the least abundant.

Significantly, alteration of the solvent composition for pyridine/dichloromethane mixtures does result in alteration of the percentages of the four isomers of $(py)_2Fe$(DeuteroPO) that are produced as seen in Table 1. However, the percentage of the α-isomer of the iron oxophlorin that forms is reduced when such mixtures are employed as the reaction medium. Nevertheless, these results are important because they demonstrate that the regiospecificity of this oxidative process is under the control of environmental factors. Thus the protein environment provided by heme oxygenase directs the specificity of the initial oxidative attack upon the heme by control of a combination of steric and electronic effects. Very recent work has demonstrated that the regiospecificity of heme oxygenase can be altered by mutagenisis of a conserved arginine residue.[50]

Experimental Section

Materials. Iron^{III}octaethylporphyrin chloride was purchased from Mid Century. Etio-1 porphyrin, deuteroporphyrin IX dimethyl ester, protoporphyrin IX dimethyl ester, and meso porphyrin IX dimethyl ester were purchased from Porphyrin Products. Deuteroporphyrin IX-

(45) Balch, A. L.; La Mar, G. N.; Latos-Grażyński, L.; Renner, M. W.; Thanabal, V. *J Am. Chem. Soc.* **1985**, *107*, 3003.
(46) Poulos, T. L. In *The Pophyrin Handbook*; Kadish, K. M., Smith, K. M., Guillard, R., Eds; Academic Press: New York, 2000; Vol. 4, p 189.
(47) Chin, D. H.; Balch, A. L.; La Mar, G. N. *J. Am. Chem. Soc.* **1980**, *102*, 1446.
(48) Groves, J. T.; Haushalter, R. C.; Nakamura, M.; Nemo, T. E.; Evans, B. J. *J. Am. Chem. Soc.* **1981**, *103*, 2884.
(49) Weiss, R.; Gold, A.; Trautwein, A. X.; Terner, J. In *The Pophyrin Handbook*; Kadish, K. M., Smith, K. M., Guillard, R., Eds.; Academic Press: New York, 2000; Vol. 4, p 189.
(50) Zhou, H.; Migita, C. T.; Sato, M.; Sun, D.; Zhang, X.; Ikeda-Saito, M.; Fujii, H.; Yoshida, T. *J. Am. Chem. Soc.* **2000**, *122*, 8311.

d_2 dimethyl ester was prepared via a standard route using resorcinol-d_2.[51] Iron(III) was inserted into these porphyrins by a standard procedure.[52] Bis(pyridine)iron^{II}porphyrins were prepared by reduction of the appropriate iron(III) complex with zinc amalgam in pyridine solution in a controlled atmosphere drybox under purified dinitrogen. Hydrogen peroxide, 50 wt % in water, was purchased from Aldrich. Dioxygen was removed from the hydrogen peroxide samples by five freeze/pump/thaw cycles.

Reactions with H_2O_2. In a controlled atmosphere (glove) box filled with dinitrogen, a dioxygen-free pyridine-d_5 solution of the bis(pyridine)iron^{II}porphyrin (3−4 μmol) was placed in an NMR tube and sealed with a rubber septum and Parafilm. The solutions were cooled to −30 °C in an ethanol/liquid dinitrogen bath. Hydrogen peroxide/pyridine-d_5 solutions (1:60, v/v) were added via a microsyringe at −30 °C to the porphyrin solutions to give hydrogen peroxide concentrations in the range of 4−6 μmol. The progress of the reaction was followed by ^{1}H NMR spectroscopy. Mixed solvent samples were prepared in the above manner.

Instrumentation. ^{1}H NMR and 1D NOE difference spectra were recorded on a Bruker Avance 500 FT spectrometer (^{1}H frequency is 500.1100 MHz). The spectra were recorded over a 100-kHz bandwidth with 32K data points and a 5-μs 90° pulse. For a typical spectrum, between 500 and 1000 transients were accumulated with a 250-ms repetition time. The residual ^{1}H resonances of the solvent, pyridine-d_5, were used as a secondary chemical shift reference.

1D NOE difference spectra were acquired by interleaving eight scans in which the peak of interest was irradiated with eight scans off resonance and using phase cycling to generate a difference spectrum. A total of 3840 scans per spectrum were collected with a 150-ms irradiation time and a recycle time of 320 ms. Data were apodized with 40 Hz line broadening.

Acknowledgment. We thank the NIH (Grant GM-26226, A.L.B.) and the Foundation for Polish Science (L.L.-G.) for financial support and the NSF (Grant OSTI 97-24412) for partial funding of the 500-MHz NMR spectrometer.

Supporting Information Available: 1D NOE difference spectra of $(py)_2Fe^{II}$(OEP) and $(py)_2Fe^{II}$(Etio-1P) (PDF). This material is available free of charge via the Internet at http://pubs.acs.org.

JA0016405

(51) Fuhrhop, J.-H.; Smith, K. M. In *Porphyrins and Metalloporphyrins*; Smith, K. M., Ed.; Elsevier Scientific Publishing Co.: New York, 1975; p 65.

(52) Adler, A. D.; Longo, F. R.; Kampas, F. *J. Inorg. Nucl. Chem.* **1970**, *32*, 2443.